Journal of Molecular Structure 1005 (2011) 113–120

Contents lists available at SciVerse ScienceDirect

Journal of Molecular Structure

journal homepage: www.elsevier.com/locate/molstruc

Synthesis, crystal, computational study and *in vitro* anti-tuberculosis activity of *N*-(furan-2-yl-methyl)-*N*-(phenyl(quinolin-3-yl)methyl) acetamide derivatives

Yuefei Bai [a], Lijuan Wang [b], Yu Chen [c], Lei Yuan [a], Wei Xu [d], Tiemin Sun [a,*]

[a] Key Laboratory of Original New Drug Design & Discovery Ministry of Education, School of Pharmaceutical Engineering, Shenyang Pharmaceutical University, Shenyang 110016, PR China
[b] State Key Laboratory of Supramolecular Structure and Materials, Jilin University, Changchun 130012, PR China
[c] School of Vocational and Technical, Shenyang Pharmaceutical University, Shenyang 110026, PR China
[d] School of Life Science and Biopharmaceutics, Shenyang Pharmaceutical University, Shenyang 110016, PR China

ARTICLE INFO

Article history:
Received 8 April 2011
Received in revised form 15 August 2011
Accepted 16 August 2011
Available online 31 August 2011

Keywords:
One-pot synthesis
X-ray diffraction
DFT calculations
Molecular structure
Diarylquinoline

ABSTRACT

A one-pot synthesis of *N*-((6-bromo-2-methoxyquinolin-3-yl)(phenyl)methyl)-*N*-(furan-2-yl-methyl)-2-morpholinoacetamide (**1**) and *N*-((6-bromo-2-methoxyquinolin-3-yl)(phenyl)methyl)-*N*-(furan-2-yl-methyl)-2-adamantylacetamide (**2**) was achieved in good yield for the first time. Compounds **1** and **2**·H_2O were characterized by single crystal X-ray diffraction in solid state. The structures of two new derivatives have been confirmed by typical spectroscopic techniques, namely IR, ^1H and ^{13}C NMR. The optimized geometric bond lengths and bond angles obtained by using density functional theory (DFT) have been compared with X-ray diffraction values. The experimental molecular structures are well reproduced by the computation. The geometrical parameters of the title compounds are similar to those of some reported derivatives. In addition, *in vitro* anti-tuberculosis activities of derivatives **1** and **2** were also investigated.

1. Introduction

Most quinoline derivatives are of considerable interest in the field of agriculture, food, additives, materials, polymers, physical and environmental chemistry [1–6]. It is also an accepted pharmacophore and represents an important synthetic precursor in drug discovery. At the same time, some quinoline derivatives have potent anti-tumor, anti-bacterial, anti-ulcer, anti-platelet aggregation [7–10], anti-inflammatory activities and especially show good activity against mycobacterial growth [11]. It is estimated that approximately eight million people developed active tuberculosis (TB) in 2004 with two million death. The prevailing situation is even worse for a continuous increase in the number of immune-compromised patients living with HIV who are more prone to TB and other bacterial infections [12]. As a result, TB has been increased substantially on a worldwide basis over the past decade, but no TB-specific drugs have been discovered in the past 40 years.

A Phase II clinical trial of anti-tubercular TMC-207 has been completed and expected to be marketed in 2012 if approved. TMC-207 acts on a new target at proton pump of adenosine triphosphate (ATP) synthase [13]. With regard to developing potent, selective and less toxic anti-tuberculosis drugs, we have published some good results from our medicinal chemistry research of diarylquinoline derivatives, such as *N*-[(6-bromo-2-methoxy-3-quinolyl)-phenylmethyl]-2-morpholino-*N*-(1-phenylethyl) acetamide [14], *N*-((6-bromine-2-methoxylquinoline-3-yl)benzyl)-3-morpholine-*N*-(naphthalene-1-yl)propionamide [15] and *N*-(naphthalen-1-yl)-*N*-(phenyl(quinolin-3-yl)methyl) amide derivatives [16]. According to literature survey, mefloquine, a well known anti-malarial drug, was identified as an agent with relatively potent activity against nonreplicating persistent TB (NRP-TB). There are data suggestive of an ATPase target for mefloquine-based compounds. A remarkable similarity of mefloquine to TMC-207 was found when it was superimposed with TMC-207. Mao et al. [17] replaced hydroxyl group with C—N double bond and obtained derivative **I** whose anti-TB activity is better than or equal to that of mefloquine while demonstrating significantly less toxicity at a receptor, cellular, and animal level. Considering the acid amide-enol tautomerization, we replaced hydroxyl with acid amide (Scheme 1). At the same time, furan, morpholine and adamantine are also good moiety with anti-tuberculosis activity. We introduced morpholine to form hydrogen bonds with Glu-61 in the c-subunit of ATP synthase and prevent proton transport that is an essential step in the synthesis of ATP [17]. Meanwhile adamantine is incorporated to get better lipophilicity and higher selectivity. On the basis of the aforementioned features,

* Corresponding author. Tel./fax: +86 24 23986398.
E-mail address: suntiemin@126.com (T. Sun).

0022-2860/$ - see front matter © 2011 Elsevier B.V. All rights reserved.
doi:10.1016/j.molstruc.2011.08.033

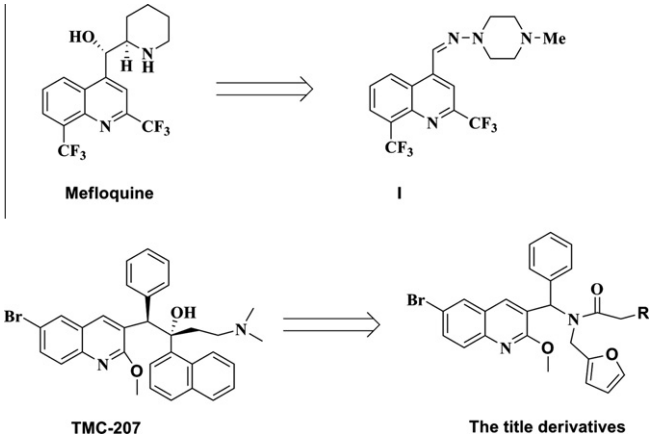

Scheme 1. The proposed design idea of TMC-207 derivatives.

N-((6-bromo-2-methoxyquinolin-3-yl) (phenyl)methyl)-*N*-(furan-2-yl-methyl)-2-morpholinoacetamide (**1**) and *N*-((6-bromo-2-methoxyquinolin-3-yl) (phenyl)methyl)-*N*-(furan-2-yl-methyl)-2-adamantylacetamide (**2**) were synthesized in one- pot method, instead of other common stepwise synthesis [18], and confirmed by spectroscopy techniques. The syntheses of the derivatives **1** and **2** have never been reported before. In addition, the organic molecular structures of the two derivatives in the ground state were optimized by a DFT method. It is well known that DFT has become the dominant and accurate computational tools for dealing with natural organic molecules [19]. The computation is valuable for providing insight into diarylquinoline derivatives with potent anti-tuberculosis activity.

2. Experimental and computational details

2.1. Experimental

The melting points were determined using a Gallenkamp apparatus. By using a Perkin Elmer one FT-IR spectrograph with KBr pallets, the IR spectra of the two derivatives were recorded in the range of 4000–400 cm^{-1} region. With the Bruker NMR spectrometer, using tetramethylsilane (TMS) as internal standard and $CDCl_3$ as solvent, the ^1H and ^{13}C NMR spectra were recorded. Combustion gas chromatography method was used for elemental analysis, and these analyses were performed on a Hewlett–Packard 185 CHN analyzer. Mass spectrometry (MS): Hewlett–Packard 1100 LC/MSD spectrometer (Hewlett–Packard, USA); X-ray spectra of the selected crystal **1** with dimensions of 0.25 × 0.22 × 0.13 mm and **2**·H_2O with dimensions of 0.32 × 0.24 × 0.22 mm were recorded by Bruker P4 X-diffractometer. Data were collected by using graphite monochromated MoKα radiation (λ = 0.71073 Å) at 293 K. For **1** and **2**·H_2O, data collection: APEX2 [20]; cell refinement: SAINT [21]; program used to solve structure: SHELXS-97 [22]; program used to refine structure, calculate the hydrogen bonds and draw molecular figures: SHELXTL-97 [23]; program used to measure centroid-centroid distance: Mercury 2.3 [24].

2.2. Preparation of *N*-((6-bromo-2-methoxyquinolin-3-yl) (phenyl) methyl)-*N*-(furan-2-yl-methyl)-2-morpholinoacetamide (**1**)

Triethylamine and dimethylformamide (DMF) (Aldrich, Co. Ltd.) were purchased and used after dehydrated with molecular sieves 4 Å. Morpholine, tetrabutylammonium iodide (TBAI), 1-adamantanamine hydrochloride and 2-chloroacetyl chloride (Wako Co. Ltd.) were purchased. All the reagents were of analytical grade and are commercially available. For TLC analysis, pre-coated plates of silica gel 60 F254 were used. Spots were visualized with UV light and iodide vapors.

To a stirred solution of 1-(6-bromo-2-methoxyquinolin-3-yl)-*N*-(furan-2-yl-methyl)-1-phenylmethanamine (0.630 g, 1.5 mmol) preparated according to the modified literature method [25] and dry triethylamine (0.455 g, 0.15 mmol) in dry DMF (20 mL) at −20 °C was added 2-chloroacetyl chloride (0.178 g, 1.575 mmol) diluted with 5 mL dry DMF under nitrogen atmosphere until no starting material could be detected via TLC. With no further purification necessary, then morpholine (0.131 g, 1.5 mmol) and tetrabutylammonium iodide (0.055 g, 0.15 mmol) were added to the above solution. After stirring for 7 h at 60 °C, the reaction mixture was quenched with water then extracted with chloroform. The resulting organic phase was then dried over anhydrous magnesium sulfate, concentrated at reduced pressure and the residue was separated by flash column chromatography (50% ethyl acetate in hexane) for purification, obtaining a white powder 0.562 g in a yield of 68.2%, m.p. 217–219 °C (Scheme 2).

IR(KBr pellets)/cm^{-1}: 2928, 2852(NCH_2), 1649(C═O), 1623, 1598, 1465(ArH), 1257, 1010, 1111(C—O).

^1H NMR (500 MHz, $CDCl_3$) δ: 2.47–2.57(m, 4H, 2×NCH_2); 3.28 (d, 1H, J = 13.5 Hz, COC H_2-β); 3.42(d, 1H, J = 13.5 Hz, $COCH_2$-α); 3.44–3.47(m, 4H, 2×OCH_2); 3.89(s, 3H, OCH_3); 4.12(d, J = 15.5 Hz, 1H, NCH_2); 4.94(d, J = 15.5 Hz, 1H, NCH_2); 5.75(s, 1H, furan-H20); 6.02(s, 1H, furan-H21); 7.05(s, 1H, ArCH); 7.13–7.14(m, 2H, C_6H_5-H2, H6); 7.26–7.28(m, 1H, C_6H_5-H4); 7.35–7.37(m, 2H, C_6H_5-H3, H5); 7.37(s, 1H, quinoline ring-H7); 7.38–7.39(m, 1H, quinoline ring-H2); 7.64–7.65(m, 1H, quinoline ring-H3); 7.68(s, 1H, furan-H22); 7.72–7.73(m, 1H, quinoline ring-H6).

^{13}C NMR (125 MHz, $CDCl_3$) δ:170.4, 160.4, 150.1, 144.7, 141.8, 137.3, 136.7, 133.0, 129.6, 129.4, 128.8, 128.5, 128.3, 128.1, 127.7, 126.4, 125.9, 117.4, 110.3, 110.2, 62.2, 57.3, 40.7, 53.9, 53.6, 53.6, 66.5, 66.5.

MS (ESI(+)): m/z 550.2 $[M+H]^+$, 552.2 $[M+2+H]^+$. Anal. calc. for $C_{28}H_{28}BrN_3O_4$: C, 61.10; H, 5.13; N, 7.63. Found: C, 61.09; H, 5.15; N, 7.65.

2.3. *N*-((6-bromo-2-methoxyquinolin-3-yl)(phenyl)methyl)-*N*-(furan-2-yl-methyl)-2-adamantylace-tamide (**2**)

In the similar manner as described above, derivative **2** was obtained as a white solid (0.9765 g, 65.1%), m.p. 252–255 °C.

IR (KBr pellets)/cm^{-1}: 3432(NH), 2902, 2847(adamantyl group), 1650(C═O), 1625, 1601, 1464(ArH), 1254, 1013(C—O).

^1H NMR (500 MHz, $CDCl_3$) δ: 1.51–2.09(m, 15H, adamantyl group); 3.46(d, 1H, J = 13.5 Hz, $COCH_2$-β); 3.74(d, 1H, J = 13.5 Hz, $COCH_2$-α); 3.96(s, 3H, OCH_3); 4.09(d, J = 15.5 Hz, 1H, NCH_2); 5.00(d, J = 15.5 Hz, 1H, NCH_2); 5.70(s, 1H, furan-H20); 6.03(s, 1H, furan-H19); 7.09(s, 1H, ArCH); 7.15–7.16(m, 2H, C_6H_5-H2, H6); 7.30–7.32(m, 1H, C_6H_5-H4); 7.39–7.41(m, 2H, C_6H_5-H3, H5); 7.39(s, 1H, quinoline ring-H7); 7.40–7.41(m, 1H, quinoline ring-H2); 7.64–7.65(m, 1H, quinoline ring-H3); 7.68(s, 1H, furan-H18); 7.72–7.73(m, 1H, quinoline ring-H6).

^{13}C NMR (125 MHz, $CDCl_3$) δ: 170.4, 160.3, 150.1, 144.7, 142.0, 137.7, 136.7, 133.2, 129.7, 129.5, 128.7, 128.6, 128.3, 128.2, 127.8, 126.4, 126.0, 117.5, 110.6, 110.2, 58.5, 54.0, 53.9, 40.7, 51.1, 42.0, 41.9, 41.8, 36.5, 36.5, 36.5, 29.4, 29.4, 29.4.

MS (ESI(+)): m/z 614.2 $[M+H]^+$, 615.2 $[M+2]^+$. Anal. calcd for $C_{34}H_{36}BrN_3O_3$: C, 66.45; H, 5.90; N, 6.84. Found: C, 66.42; H, 5.94; N, 6.90.

2.4. Computational methods

Molecular structures of the two new derivatives **1** and **2** in the ground state were optimized by DFT method using Becke's three

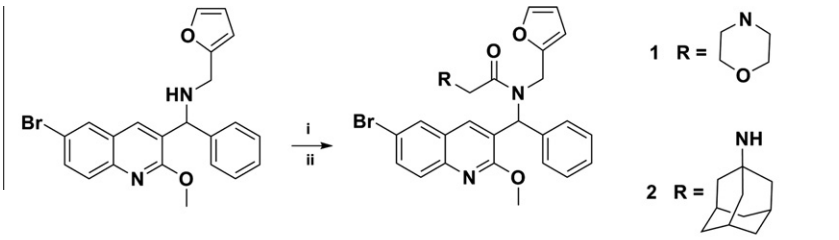

Reagents and conditions:

(i) 2-chloroacetyl chloride, Et_3N, DMF, N_2 atmosphere, at -20℃.

(ii) morpholine or 1- adamantanamine hydrochloride, DMF, at heated 60℃.

Scheme 2. A one-pot synthesis of novel derivatives **1** and **2**.

parameter hybrid exchange-correlation functional in conjunction with a 6-31++G** basis set [26]. Molecular geometries were fully optimized by Berny's optimization algorithm using redundant internal coordinates. The entire set of computation was performed using the GAUSSIAN 09W™ software [27]. An extensive search for low energy conformations on potential energy surfaces (PES) of compounds was carried out and minimum energy conformations were re-optimized at DFT/B3LYP/6-31++G** without symmetry constraints. For large and flexible molecules, the PES contains many local minima corresponding to different relative orientations of the functional groups in the molecules. The calculated results at the same level show that there are no imaginary frequencies for both derivatives, indicating that both of them are equilibrium geometries. The computational molecular structures were shown by the animation option of the Gauss-View5.0™ graphical interface [28].

2.5. Determining the minimal inhibitory concentration (MIC)

A series of broth tubes containing diluted chemical synthetic compound concentrations were prepared and inoculated with a 48 h liquid culture of *Mycobacterium phlei* 1180. Then the tubes were incubated at 37 °C for 20 h. The MIC was defined as the lowest concentration that prevented the mycobacterial growth and their inhibition against other strains is under test.

3. Results and discussion

3.1. Crystal structure determination of derivatives *1* and *2*·H_2O

The crystals of **1** and **2**·H_2O were grown from slow evaporation of water/ethanol mixed solvent at ambient conditions. Derivative **1** is in monoclinic crystal system with C 2/c space group, unit cells a = 32.666(6) Å, b = 10.737(2) Å, c = 17.161(3) Å. While **2**·H_2O is in trigonal crystal system, R-3 space group with one additional free water molecule, unit cells a = 34.5748(12) Å, b = 34.5748(12) Å, c = 13.4496(4) Å. The crystallographic and refinement data of **1** and **2**·H_2O are shown in Table 1.

3.2. Crystal structure descriptions of *1* and *2*·H_2O

In the molecular structure **1**: The bond lengths Br(1)—C(1) (1.881 Å) and C(9)—O(1) (1.357 Å) are characteristics of single bond. C(23)—O(2) (1.217 Å) is characteristics of the bond length in a carbonyl group. The bond angle C(6)—C(1)—Br(1) is 121.1°. The bond length C(23)—N(2) is 1.367 Å. The bond angles

Table 1
Crystal data and refinement details for **1** and **2**·H_2O.

Derivatives	**1**	**2**·H_2O
Empirical formula	$C_{28}H_{28}BrN_3O_4$	$C_{34}H_{36}BrN_3O_3{\cdot}H_2O$
Formula weight	550.43	632.58
Crystal size	0.25 × 0.22 × 0.13	0.32 × 0.24 × 0.22
Crystal color	Colorless	Colorless
Crystal system	Monoclinic	Trigonal
Space group	C 2/c	R-3
a (Å)	32.666(6)	34.5748(12)
b (Å)	10.737(2)	34.5748(12)
c (Å)	17.161(3)	13.4496(4)
α (°)	90.00	90.00
β (°)	120.43(3)	90.00
γ (°)	90.00	120.00
V (Å^{-3})	5190(2)	13923.8(8)
Z	8	18
Theta range for data collection (°)	3.11–25.01	1.66–25.02
Limiting indices	$-38 \leqslant h \leqslant 38$, $-12 \leqslant k \leqslant 12$, $-20 \leqslant l \leqslant 20$	$-41 \leqslant h \leqslant 27$, $-41 \leqslant k \leqslant 40$, $-15 \leqslant l \leqslant 16$
Reflections collected/unique	20,083/4574 (R_{int} = 0.0391)	26,541/5430 (R_{int} = 0.0623)
Refined parameters/restraints	326/0	394/19
Goodness of Fit on F^2	1.054	0.937
R_1, wR_2	0.0649, 0.2270	0.0577, 0.1926
Data completeness	0.998	0.997
Data/restraints/parameters	4574/0/326	5430/19/394
Max. and min. transmission	0.8102 and 0.6731	0.7402 and 0.6810
Largest diff. peak and hole (eÅ^{-3})	0.495 and −0.783	0.320 and −0.862

O(2)—C(23)—N(2)and O(2)—C(23)—C(24) are 121.8° and 119.3° respectively. The morpholine system exists in a twisted chair-like conformation and the bond angles indicate sp^3 hybridization nature of those atoms. The torsion angles C(8)—C(9)—N(1)—C(4) and C(20)—C(19)—O(4)—C(22) are −1.1° and −1.2°, which means that substituted quinoline and furan remain almost planar individually. The dihedral angle between passing through the atoms of substituted quinoline and benzene planes is 99.1°. It is almost perpendicular with respect to one another. The dihedral angle between passing through the atoms of substituted quinoline and furan planes is 15.1 l°. It is generally parallel to one another. Moreover, the systems of morpholine and benzene are inclined to one another.

We have analyzed the hydrogen bond interactions in the molecular crystal structure **1**, **2**·H_2O and their geometry and details of interactions in the structures are listed in the Table 2. No conventional hydrogen bonds were found at 293(2)K for **1**. The weak intermolecular hydrogen bond C(22)—H(22)···O(2)^{i} (i = −*x*, −*y* + 2, −*z*) is observed, as is shown. In addition to the interactions described above, the crystal can be stabilized by weak π-stacking interactions between the planes of the π-electron systems of substituted quinoline and furan with a ring centroid-centroid distance of 3.819 Å [30]. The two-dimensional layer structure is formed in the crystal packing from Fig. 3. Interestingly, the crystal packing of molecule **1** is a C(28)—H(28A)···π intramolecular contact with a short H···X distance of 2.786 Å calculated by Mercury 2.3 [24] and they are in a nearly perpendicular orientation, which brought about the peculiar packing motif (X is the center of the benzene ring) [30].

Similarly, in the molecular structure **2**·H_2O: the free water molecule has two positions owing to the crystallographic disorder of O(1W) and O(1W′). Each of them has 50% occupancy over the two positions. The bond length C(23)—N(2) is 1.351 Å. The bond angle C(6)—C(1)—Br(1) is 120.2°. The bond angles O(3)—C(23)—N(2) and O(3)—C(23)—C(24) are 122.0° and 120.1° respectively. The bond angles of amantadine system also indicate sp^3 hybridization nature of those atoms. The torsion angles C(8)—C(9)—N(1)—C(4) and (20)—C(21)—O(2)—C(18) are −0.7°, 0.2° respectively. The dihedral angle between passing through the atoms of substituted quinoline and benzene planes is 69.6°. The dihedral angle between passing through the atoms of substituted quinoline and furan planes is 27.3°. While the dihedral angles between phenyl and substituted quinolinyl groups in related structure TMC-207 is 97.4°, naphthalenyl and substituted quinolinyl groups are nearly coplanar [14]. At the same time, there is a strong intermolecular hydrogen bond O(1W)—H(1W)···O(1W)^{ii}, O(1W′)—H(1W)···O(1W')^{ii} (ii = *x* − *y* + 2/3, *x* + 1/3, −*z* + 1/3). and C(7)—H(7)···O(3)^{iii} (iii = *x* − *y* + 2/3, *x* + 1/3, −*z* + 4/3) is also observed in the crystal packing (Table 2).

The crystal with a ring centroid-centroid distance of 4.199 Å between substituted quinoline and furan plane is indicative of a weak π-stacking stabilization. Those interactions are fairly important in view of the stability of the crystal structure. The three-dimensional supramolecular network structure is assembled by the hydrogen bond interactions (Fig. 4).

As is above described, these two derivatives are analogous to some previously reported compounds [13–16,29,31]. All of them belong to diarylquinoline with the comprising of 3-benzyl-6-bromo-2-methoxyquinoline and amido chain. The maximum difference in experimental bond lengths between these two derivatives is the furan group. It can be attributed to steric repulsion.

Table 2
Hydrogen bond geometry (Å, °) for crystal **1** and **2**·H_2O.

D—H···A	d(D—H)	d(H···A)	d(D···A)	<(DHA)
Crystal **1**				
C(22)—H(22)···O(2)^{i}	0.93	2.52	3.428(9)	165.9
Crystal **2**·H_2O				
O(1 W)—H(1 WA)···O(1 W)^{ii}	0.87	2.05	2.77(2)	138.8
O(1 W)—H(1 WB)···N(3)	0.87	2.14	2.913(18)	147.1
O(1 W′)—H(1WC)···O(1W′)^{ii}	0.87	1.87	2.719(12)	164.9
O(1W′)—H(1WD)···N(3)	0.89	2.31	2.936(12)	127.8
C(7)—H(7)···O(3)^{iii}	0.93	2.42	3.240(4)	147.3
C(24)—H(24B)···O(2)	0.97	2.50	3.298(5)	139.5

Symmetry codes: (i) −*x*, −*y* + 2, −*z*; (ii) *x* − *y* + 2/3, *x* + 1/3, −*z* + 1/3; (iii) *x* − *y* + 2/3, *x* + 1/3, −*z* + 4/3.

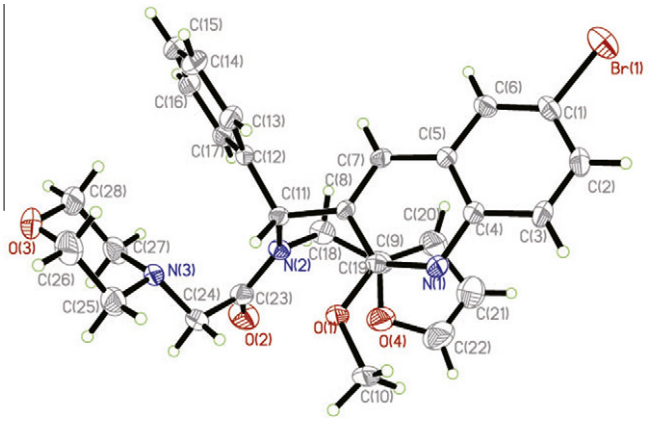

Fig. 1. The molecular structure with atom-numbering scheme of derivative **1** displacement ellipsoids is drawn at the 30% probability level.

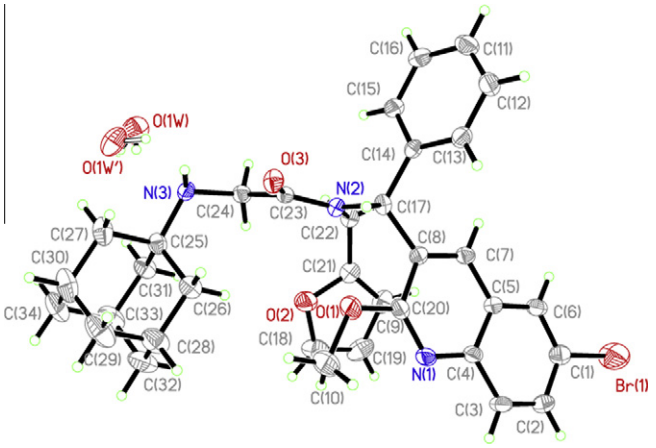

Fig. 2. The molecular structure with atom-numbering scheme of derivative **2**·H_2O displacement ellipsoids are drawn at the 30% probability level.

3.3. Geometry optimization

The calculated molecular structures of **1**, **2** and their numbering scheme are shown in Figs. 5 and 6, in accordance with the atom numbering given in Figs. 1 and 2 respectively. The global energy minimum obtained by DFT calculations of the structure optimization for **1** and **2** are – 4120.770849 Hartree (-25.86×10^5 kcal mol^{-1}) and – 4279.0657667 Hartree (-26.85×10^5 kcal mol^{-1}) respectively. The optimized structural parameters of **1** and **2** calculated using B3LYP functional with a 6-31++G** basis set are listed and compared with X-ray diffraction values in Table 3.

The corresponding distances of C(23)—N(2) in the optimized geometry of two molecules are 1.378 Å and 1.382 Å, respectively. As expected, most of the calculated bond lengths for the two derivatives are slightly larger than the X-ray values. For the optimized

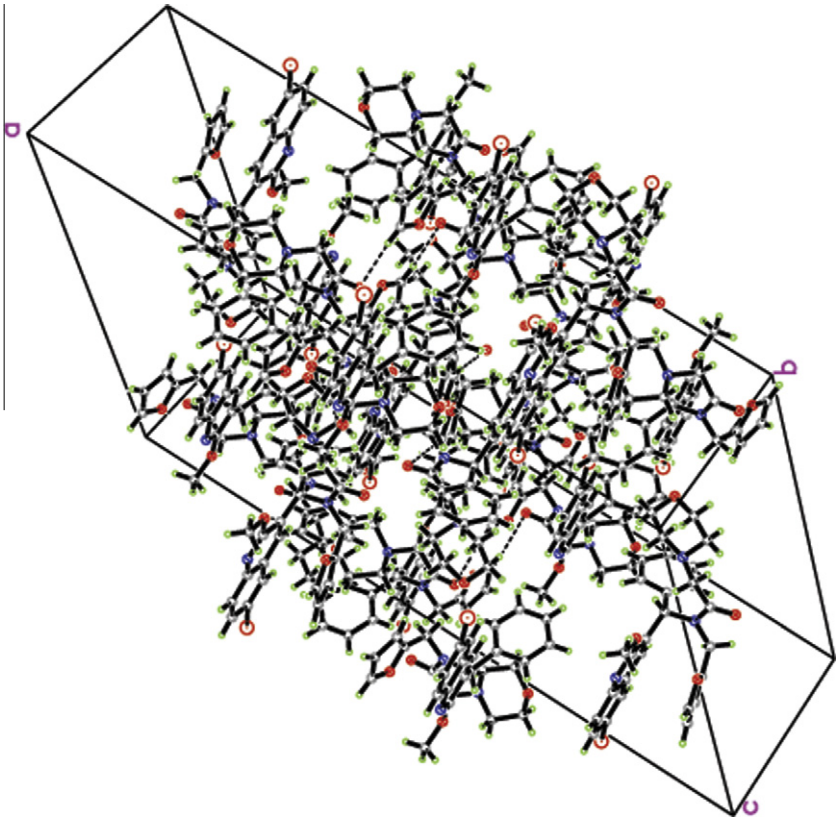

Fig. 3. Crystal packing structure of **1**.

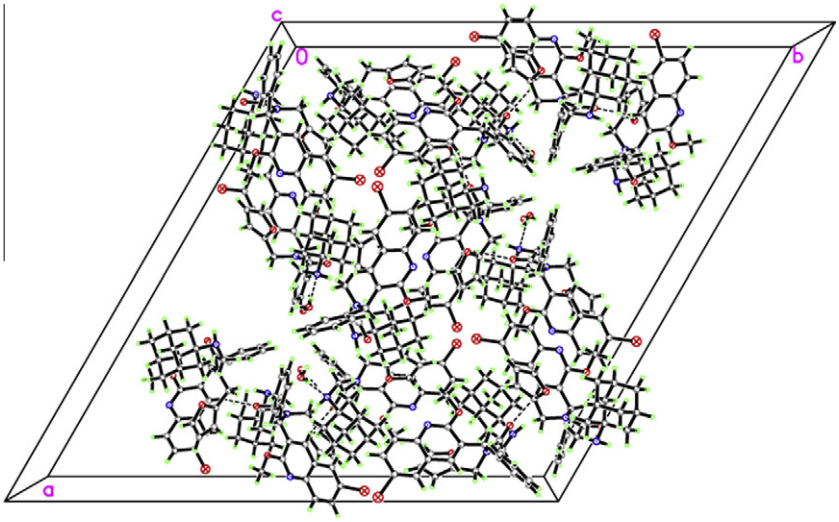

Fig. 4. Crystal packing structure of **2**·H_2O.

geometry of **1** in the ground state with C1 symmetry, the calculated bond lengths and bond angles deviate from the X-ray values by 0.09 Å at C(21)—C(22) and 2.7° at O(2)–C(23)–C(24), respectively. In contrast, the optimized geometry of **2** in the ground state with C1 symmetry shows a maximum difference from the X-ray values in bond lengths and bond angles of 0.09 Å at C(19)—C(20) and 2.2° at C(8)—C(17)—C(14), respectively.

These deviations may be partly due to the fact that the theoretical optimization for a single molecule is obtained in the gas phase (*in vacuo*) without any intermolecular interactions. However the experimental data are measured at very low temperature in the solid phase where it can undergo intermolecular and crystal packing effects interactions holding the molecules together as stated above, so the molecular rotations were restricted.

In addition, the optimized structure predicts boat conformation as the preferential one to morpholinyl group for **1**. At the same time, the optimized conformations of furan group are also slight different from X-ray data for **1** and **2**·H_2O respectively. The difference also exists in structure of 4-[(2-{[(2-furylmethyl)-imino]methyl}-4-methoxyphenoxy)methyl]benzonitrile [32].

The conformations of investigated molecules are mainly restrained by hydrogen bonds and electrostatic interactions. In

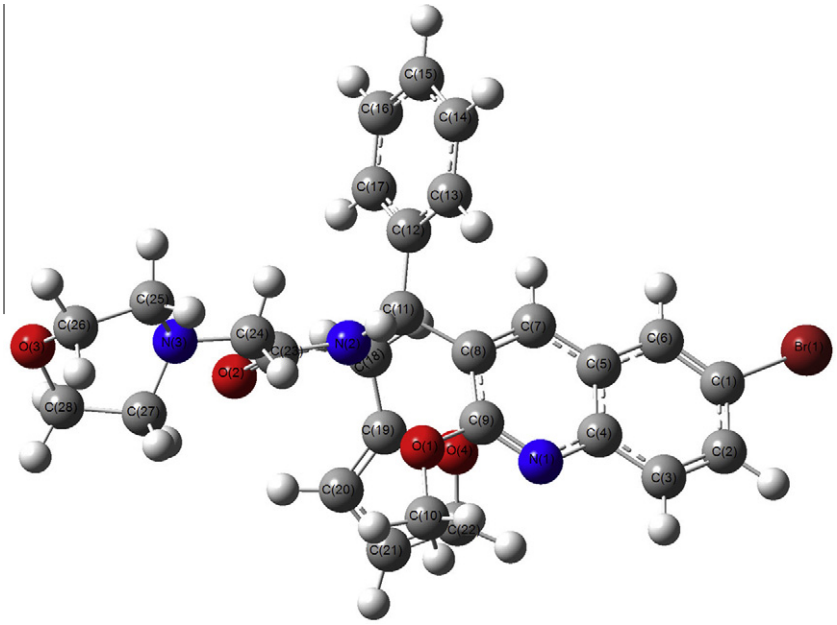

Fig. 5. Atom numbering and optimized structure of **1** from B3LYP/6-31++G** calculation.

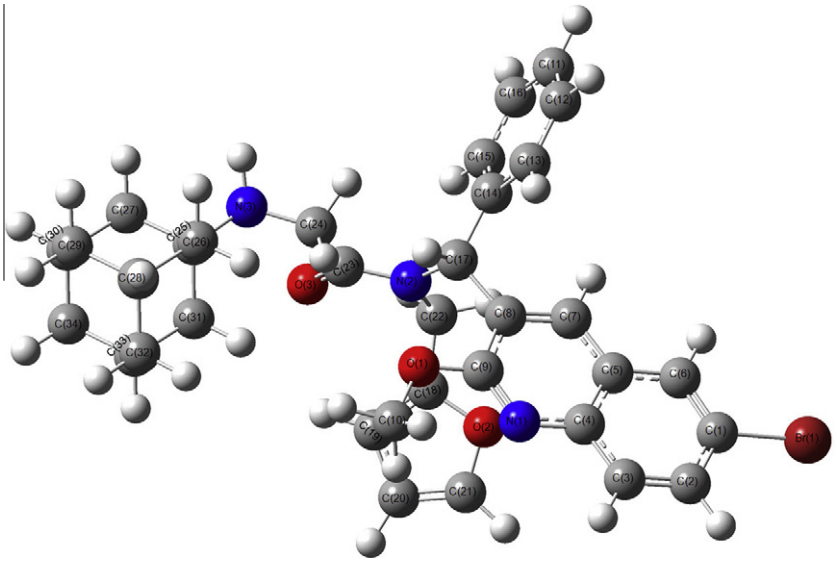

Fig. 6. Atom numbering and optimized structure of **2** from B3LYP/6-31++G** calculation.

crystals, there are both intramolecular and intermolecular electrostatic interactions. While in the optimized single molecule, the intermolecular interactions are absent, and the intramolecular ones are stronger than those in crystals. The variations of intermolecular interactions from crystal to single molecules should be responsible for the above described geometry differences. The observed disagreement between computation and experiment could be a consequence of the anharmonicity and the general tendency that quantum chemical methods overestimate the force constants at the exact equilibrium geometry.

3.4. Anti-tuberculosis activity

To qualify as a drug candidate, a new molecule has to be analyzed for the parameters set by Lipinski's rule of five using Osiris property explorer (www.organic-chemistry.org). Lipinski's rule of five is a rule of thumb to evaluate drug likeliness or to determine if a compound with a certain pharmacological or biological activity has properties that would make it a likely orally active drug in humans. The rule is important for drug development where pharmacologically active lead structure is optimized step wise for increased activity and selectivity, as well as drug like properties as described. The rule states that in general an orally active drug has not more than 5 hydrogen bond donors, and not more than 10 hydrogen acceptors, a molecular weight under 500 and the partition coefficient $c\log P$ less than 5 [33]. The two derivatives fall well in the range, but their molecular weight values and the high lipophilicity of derivative **2** ($c\log P = 6.10$) violate Lipinski's Rule of Five, which may limit its therapeutic potential (Table 4). In the case of anti-tubercular activity studies, although both were found biologically active, the unsatisfactory result is that both showed lower inhibitory activities than the standard drugs. In addition to the above stated, we assume that steric factor should account for the weak activity of derivative **2**. Adamantyl group is rigid and

Table 3
Selected experimental and calculated geometry parameters for crystal **1** and **2**·H_2O.

Bond distances (Å)	Exp. (**1**)	Cal.	Dif.	Bond distance (Å)	Exp. (**2**·H_2O)	Cal.	Dif.
Br(1)—C(1)	1.881	1.907	0.03	C(1)—Br(1)	1.887	1.907	0.02
C(1)—C(2)	1.399	1.412	0.01	C(1)—C(2)	1.401	1.412	0.01
C(2)—C(3)	1.361	1.381	0.02	C(2)—C(3)	1.353	1.381	0.03
C(3)—C(4)	1.416	1.417	0.00	C(3)—C(4)	1.430	1.417	−0.01
C(4)—C(5)	1.416	1.426	0.01	C(4)—C(5)	1.405	1.426	0.02
C(5)—C(6)	1.413	1.416	0.00	C(5)—C(6)	1.399	1.417	0.02
C(1)—C(6)	1.357	1.377	0.02	C(1)—C(6)	1.359	1.377	0.02
C(5)—C(7)	1.417	1.423	0.01	C(5)—C(7)	1.433	1.423	−0.01
C(7)—C(8)	1.361	1.371	0.01	C(7)—C(8)	1.357	1.371	0.01
C(8)—C(9)	1.436	1.440	0.00	C(8)—C(9)	1.437	1.440	0.00
C(9)—N(1)	1.294	1.308	0.01	C(9)—N(1)	1.304	1.308	0.00
C(9)—O(1)	1.357	1.353	0.00	C(9)—O(1)	1.343	1.353	0.01
C(10)—O(1)	1.438	1.437	0.00	C(10)—O(1)	1.441	1.437	0.00
C(8)—C(11)	1.518	1.527	0.01	C(8)—C(17)	1.513	1.527	0.01
C(11)—C(12)	1.521	1.534	0.01	C(14)—C(17)	1.527	1.535	0.01
C(12)—C(13)	1.382	1.405	0.02	C(13)—C(14)	1.386	1.405	0.02
C(13)—C(14)	1.399	1.394	−0.01	C(12)—C(13)	1.392	1.395	0.00
C(14)—C(15)	1.366	1.399	0.03	C(11)—C(12)	1.374	1.399	0.03
C(15)—C(16)	1.345	1.395	0.05	C(11)—C(16)	1.363	1.395	0.03
C(16)—C(17)	1.388	1.400	0.01	C(15)—C(16)	1.390	1.400	0.01
C(17)—C(12)	1.394	1.399	0.01	C(14)—C(15)	1.382	1.399	0.02
C(11)—N(2)	1.475	1.477	0.00	C(17)—N(2)	1.485	1.475	−0.01
C(18)—N(2)	1.476	1.480	0.00	C(22)—N(2)	1.469	1.478	0.01
C(18)—C(19)	1.497	1.498	0.00	C(21)—C(22)	1.478	1.499	0.02
C(19)—O(4)	1.345	1.375	0.03	C(21)—O(2)	1.376	1.375	0.00
C(22)—O(4)	1.362	1.365	0.00	C(18)—O(2)	1.380	1.365	−0.02
C(21)—C(22)	1.275	1.363	0.09	C(18)—C(19)	1.309	1.363	0.05
C(20)—C(21)	1.434	1.435	0.00	C(19)—C(20)	1.344	1.435	0.09
C(19)—C(20)	1.332	1.366	0.03	C(20)—C(21)	1.405	1.366	−0.04
C(23)—N(2)	1.367	1.378	0.01	C(23)—N(2)	1.351	1.382	0.03
C(23)—O(2)	1.217	1.229	0.01	C(23)—O(3)	1.223	1.227	0.00
C(23)—C(24)	1.516	1.538	0.02	C(23)—C(24)	1.529	1.546	0.02
C(24)—N(3)	1.451	1.447	0.00	C(24)—N(3)	1.458	1.451	−0.01
Bond angle (°)	Exp. '(1)	Cal.	Dif.	Bond angle (°)	Exp. (2·H_2O)	Cal.	Dif.
C(6)—C(1)—Br(1)	121.1	119.7	−1.4	C(6)—C(1)—Br(1)	120.2	119.7	−0.5
N(1)—C(9)—C(8)	125.9	124.9	−1.0	N(1)—C(9)—C(8)	125.1	124.9	−0.2
C(19)—O(4)—C(22)	107.3	107.4	0.1	C(21)—O(2)—C(18)	105.8	107.4	1.6
O(1)—C(9)—C(8)	114.3	115.4	1.1	O(1)—C(9)—C(8)	114.6	115.5	0.9
C(8)—C(11)—C(12)	113.8	113.5	−0.3	C(8)—C(17)—C(14)	115.7	113.5	−2.2
O(2)—C(23)—C(24)	119.3	122.0	2.7	O(3)—C(23)—C(24)	120.1	122.2	2.1
O(2)—C(23)—N(2)	121.8	120.7	−1.1	O(3)—C(23)—N(2)	122.0	120.5	−1.5

Table 4
Anti-tubercular activity and pharmacological parameters for bioavailability of the derivatives (*M. phlei* 1180).

Entry No.	MIC (mg mL^{-1})	*c*log*P*	Drug likeliness	Drug score
1	140	4.22	1.57	0.40
2	210	6.10	1.29	0.15

Standard: isoniazid 8 mg mL^{-1}, rifampicin 10 mg mL^{-1}. All compounds tested at concentration of 1.0 mg mL^{-1}.

large in contrast with morpholinyl group. As a result, it might be difficult to penetrate mycobacterial cell wall barrier to reach the active site.

4. Conclusions

With the goal of developing better anti-tuberculosis drugs, we synthesized two new diarylquinoline derivatives by a one-pot method. The molecular structures of **1** and **2**·H_2O were determined by single crystal X-ray method. In spite of the aforementioned slightly conformational discrepancies, the optimized geometric bond lengths and bond angles obtained by using DFT are generally closer to X-ray diffraction values, which supports the solid-state structures. Hence, the computed results with only reasonable deviations from the experimental values seem feasible. The structural elucidation obtained by this paper could further contribute to understanding molecular structures of the diarylquinoline derivatives and especially discovering better anti-tubercular inhibitors.

Supplementary material

The supplementary crystallographic data for the two new derivatives reported in this paper have been deposited with the Cambridge Crystallography Data Centre, 12 Union road, Cambridge CB22 1EZ, UK (Fax: +44 1223 336 033; E-mail: deposit@ccdc.cam.ac.uk or http://www.ccdc.cam.ac.uk) and are available free of charge on request quoting the deposition number CCDC 814136, CCDC 815289 for **1** and **2**·H_2O respectively.

Acknowledgements

The authors gratefully acknowledge the College of Experimental Center of Testing Science of Jilin University for the X-ray data collection and School of Pharmaceutical Engineering, Shenyang Pharmaceutical University for providing research facilities.

References

[1] (a) Z.-Y. Yu, G.-Y. Shi, Q. Sun, H. Jin, Y. Teng, K. Tao, G.-P. Zhou, P. Guo, W. Liu, F. Wen, T.-P. Hou, Eur. J. Med. Chem. 44 (2009) 4726;
(b) V.K. Gupta, M. Alok, G. Vibha, J. Colloid Interface Sci. 284 (2005) 89.

[2] (a) M.-M. Zheng, G.-D. Ruan, Y.-Q. Feng, J. Chromatogr. A 1216 (2009) 7510;
(b) N. Adriana, L. Zdzislawa, Eur. J. Nutr. 48 (2009) 419.

[3] (a) H.-F. Li, X.-L. Xu, J.-Y. Yang, X. Xie, H. Huang, Y.-Z. Li, Tetrahedron Lett. 52 (2011) 530–533;
(b) P. Bolduc, A. Jacques, S.K. Collins, J. Am. Chem. Soc. 132 (2010) 12790;
(c) P.H. Dobbelaar, C.H. Marzabadi, Tetrahedron Lett. 51 (2010) 201.

[4] (a) J. Barluenga, M. Fañanás-Mastral, A. Fernández, F. Aznar, Eur J. Org. Chem. 10 (2011) 1961;
(b) A. Joshua, Z. Matthias, B. Christian, Org. Lett. 13 (2011) 1322;
(c) Y. Luo, X.-L. Pan, J. Wu, Org. Lett. 13 (2011) 1150.

[5] (a) A.K. Nedeltchev, H. Han, P.K. Bhowmik, L. Ma, J. Polym. Sci. Part A: Polym. Chem. 49 (2011) 1907;
(b) J.-X. Luo, C.-L. Yang, J. Zheng, J.-Y. Ma, L.-Y. Liang, M.-G. Lu, Eur. Polym. J. 47 (2011) 385;
(c) W.-A. Ma, Z.-X. Wang, Dalton Trans. 40 (2011) 1778.

[6] (a) E.H. Weyand, J. Defauw, C.A. McQueen, C.L. Meschter, S.K. Meegalla, E.J. LaVoie, Food Chem. Toxicol. 31 (1993) 707;
(b) J.F. McBride, F.J. Brockman, J.E. Szecsody, G.P. Streile, J. Contam. Hydrol. 9 (1992) 133.

[7] R. Miri, R. Motamedi, M.R. Rezaei, O. Firuzi, A. Javidnia, A. Shafiee, Arch. Pharm. 344 (2011) 111.

[8] P. Drazen, F. Andrea, M. Stjepan, Bioorg. Med. Chem. Lett. 18 (2010) 8566.

[9] H. Yoshie, M. Takaharu, J. Pharm. Pharmacol. 55 (2003) 1667.

[10] (a) Y.-P. Yang, M.-J. Cheng, C.-M. Teng, Y.-L. Chang, I.-L. Tsai, I.-S. Chen, Phytochemistry 61 (2002) 567;
(b) J.-J. Chen, Y-L. Chang, C.-M. Teng, C.-C. Su, I.-S. Chen, Planta Med. 68 (2002) 790;
(c) Y.-C. Chen, J.-J. Chen, Y.-L. Chang, C.-M. Teng, W.-Y. Lin, C.-C. Wu, I.-S. Chen, Planta Med. 70 (2004) 174.

[11] (a) N. Amit, M. Vikramdeep, M. Alpeshkumar, C. Evans, J. Rahul, Bioorg. Med. Chem. 15 (2007) 626;
(b) N. Amit, M. Alpeshkumar, J. Rahul, C. Evans, Bioorg. Med. Chem. 14 (2006) 847.

[12] (a) O.K. Onajole, P. Govender, P.D.v. Helden, H.G. Kruger, G.E.M. Maguire, I. Wiid, T. Govender, Eur. J. Med. Chem. 45 (2010) 2075;
(b) E.C. Rivers, R.L. Mancera, Drug Discov. Today 13 (2008) 1090.

[13] (a) K. Andries, Science 307 (2005) 223;
(b) A. Lilienkampf, J.-L. Mao, B.-J. Wan, Y.-H. Wang, S.G. Franzblau, A.P. Kozikowski, J. Med. Chem. 52 (2009) 2109;
(c) N. Lounis, T. Gevers, J.V.D. Berg, T. Verhaeghe, R. van Heeswijk, K. Andries, J. Clin. Microbiol. 46 (2008) 2212.

[14] Z.-Q. Cai, G. Xiong, S.-R. Li, J.-B. Liu, T.-M. Sun, Acta Crystallogr. Sec. E Struct. Rep Online 65 (2009) o1901.

[15] Z.-Q. Cai, S.-R. Li, T.-M. Sun, Chin. J. Struct. Chem. 29 (2010) 796.

[16] Z.-Q. Cai, C.-J. Zhu, Y.-X. Cui, B. Jiang, T.-M. Sun, Sci. China Ser. B – Chem. 52 (2009) 2051.

[17] J.-L. Mao, Y.-H. Wang, B.-J. Wan, A.P. Kozikowski, S.G. Franzblau, ChemMedChem 2 (2007) 1624.

[18] (a) S. Rajavel, U. Mahesh, S.-Q. Yao, Org. Lett. 8 (2006) 713;
(b) H.-Y. Liang, D.-Q. Zhang, Y. Yue, Z. Shi, S.-Y. Zhao, Arch. Pharm. 343 (2010) 114;
(c) S. Ghosh, L. Isaacs, J. Am. Chem. Soc. 132 (2010) 4445.

[19] T. Wang, Y.-F. Wu, L. Ding, Z. Chen, J. Mol. Struct. 994 (2011) 137.

[20] Bruker APEX2 Version 1.0-27, Bruker AXS Inc., Madison, Wisconsin, USA, 2005.

[21] Bruker, SADABS (Version 2.01), SMART (Version 5.603) and SAINT (Version 6.36a), Bruker AXS Inc., Madison, Wisconsin, USA, 2000.

[22] G.M. Sheldrick, SHELXTS-97 and SHELXTL-97, University of Göttingen, Germany, 1997.

[23] G.M. Sheldrick, SHELXTL, Version 5.1, Bruker AXS, Inc., Madison, Wisconcin, USA, 1997.

[24] C.F. Macrae, I.J. Bruno, J.A. Chisholm, P.R. Edgington, P. McCabe, E. Pidcock, L. Rodriguez-Monge, R. Taylor, J. van de Streek, P.A. Wood, J. Appl. Cryst. 41 (2008) 466.

[25] R.S. Upadhayaya, J.K. Vandavasi, N.R. Vasireddy, V. Sharma, S.S. Dixit, J. Chattopadhyaya, Bioorg. Med. Chem. 17 (2009) 2830.

[26] J.B. Foresman, A.E. Frisch, Exploring Chemistry with Electronic Structure Methods, second ed., Gaussian Inc., Pittsburgh, PA, 1996.

[27] M.J. Frisch, G.W. Trucks, H.B. Schlegel, G.E. Scuseria, M.A. Robb, J.R. Cheeseman, G. Scalmani, V. Barone, B. Mennucci, G.A. Petersson, H. Nakatsuji, M. Caricato, X. Li, H.P. Hratchian, A.F. Izmaylov, J. Bloino, G. Zheng, J.L. Sonnenberg, M. Hada, M. Ehara, K. Toyota, R. Fukuda, J. Hasegawa, M. Ishida, T. Nakajima, Y. Honda, O. Kitao, H. Nakai, T. Vreven, J.A. Montgomery Jr., J.E. Peralta, F. Ogliaro, M. Bearpark, J.J. Heyd, E. Brothers, K.N. Kudin, V.N. Staroverov, R. Kobayashi, J. Normand, K. Raghavachari, A. Rendell, J.C. Burant, S.S. Iyengar, J. Tomasi, M. Cossi, N. Rega, J.M. Millam, M. Klene, J.E. Knox, J.B. Cross, V. Bakken, C. Adamo, J. Jaramillo, R. Gomperts, R.E. Stratmann, O. Yazyev, A.J. Austin, R. Cammi, C. Pomelli, J.W. Ochterski, R.L. Martin, K. Morokuma, V.G. Zakrzewski, G.A. Voth, P. Salvador, J.J. Dannenberg, S. Dapprich, A.D. Daniels, O. Farkas, J.B. Foresman, J.V. Ortiz, J. Cioslowski, D.J. Fox, Gaussian 09, Revision A.1, Gaussian Inc., Wallingford, CT, 2009.

[28] A. Frish, A.B. Nielsen, A.J. Holder, Gauss View User Manual, Gaussian Inc., Pittsburg, PA, 2001.

[29] S. Petit, G. Coquerel, C. Meyer, J. Guillemont, J. Mol. Struct. 837 (2007) 252.

[30] M.L. Główka, D. Martynowski, K. Kozàowska, J. Mol. Struct. 474 (1999) 81.

[31] H. Rahmani, H. Pirelahi, S.W. Ng, Acta Crystallogr. Sec. E Struct. Rep. Online 65 (2009) o603.

[32] Ö. Alver, Z. Hayvalı, H. Güler, H. Dal, M. Şenyel, J. Mol. Struct. 991 (2011) 12.

[33] T. Taj, S.V. Raikar, R.R. Kamble, Arab. J. Chem., in press. doi: 10.1016/j. arabjc.2011.01.029.